

## Dissolution, Hydrolysis and Crystallization Behavior of Polyamide 6 in Superheated Water<sup>\*</sup>

Zhi-liang Wang<sup>a</sup>, Jia-li Xu<sup>a</sup>, Lian-jia Wu<sup>a</sup>, Xin Chen<sup>a, b</sup>, Shu-guang Yang<sup>a\*\*</sup>,  
Hui-chao Liu<sup>a</sup> and Xian-ju Zhou<sup>c</sup>

<sup>a</sup> State Key Laboratory for Modification of Chemical Fibers and Polymer Materials, College of Material Science and Engineering, Donghua University, Shanghai 201620, China

<sup>b</sup> R & D Center, Guangdong Xinhui Meida Nylon Co., LTD., Jiangmen 529100, China

<sup>c</sup> Department of Mathematics and Physics, Chongqing University of Posts and Telecommunications, Chongqing 400065, China

**Abstract** The dissolution, crystallization and hydrolysis behaviors of polyamide 6 (PA 6) in superheated water ( $140\text{ }^{\circ}\text{C} \leq T_{\text{H}} \leq 200\text{ }^{\circ}\text{C}$ ) are investigated. The hydrothermal processing of PA 6 can be divided into four regions: (I)  $T_{\text{H}} < 140\text{ }^{\circ}\text{C}$ , (II)  $140\text{ }^{\circ}\text{C} \leq T_{\text{H}} \leq 155\text{ }^{\circ}\text{C}$ , (III)  $155\text{ }^{\circ}\text{C} < T_{\text{H}} < 160\text{ }^{\circ}\text{C}$  and (IV)  $T_{\text{H}} \geq 160\text{ }^{\circ}\text{C}$ . Below  $140\text{ }^{\circ}\text{C}$ , the hydrothermal processing does not have obvious impact on PA 6. Between  $140\text{ }^{\circ}\text{C}$  and  $155\text{ }^{\circ}\text{C}$ , an annealing effect is observed that the hydrothermally treated resin shows increased melting temperature and lamellar thickness compared with the original PA 6. Between  $155\text{ }^{\circ}\text{C}$  and  $160\text{ }^{\circ}\text{C}$ , the hydrothermal processing induces both annealing and surface swelling. Above  $160\text{ }^{\circ}\text{C}$ , PA 6 dissolves fully in the superheated water. As PA 6 dissolves in the superheated water, hydrolysis takes place and becomes more prominent at higher temperatures and longer processing time. The hydrolysis induced molecular weight decrease fits an exponential decay.

**Keywords:** Nylon 6; Superheated water; Annealing; Crystallization; Hydrolysis.

### INTRODUCTION

Polyamide 6 (PA 6) is a semi-crystalline polymer prepared by ring-opening polymerization of  $\epsilon$ -caprolactam. Due to the hydrogen bonding between amide groups and dipole-dipole interaction, PA 6 has a high melting point ( $T_{\text{m}} \sim 220\text{ }^{\circ}\text{C}$ ) and dissolves only in strong polar solvents<sup>[1–3]</sup>. Compared with strong polar organic solvents, water is an environmentally acceptable, naturally abundant, and inexpensive solvent, so using water as a solvent for material processing is highly desirable<sup>[4]</sup>. However, many polymers do not dissolve in water under ambient condition. Above the ambient boiling point and below the supercritical point ( $374\text{ }^{\circ}\text{C}$ ,  $22.10\text{ MPa}$ ), water is in the superheated state that it has low dielectric constant, weak hydrogen bonding and high mobility, and thus water can be used as a solvent for polymer processing<sup>[5–7]</sup>.

Mathot and co-workers reported that PA 6 can dissolve in superheated water with weight content as high as  $70\text{ wt}\%$ <sup>[8–10]</sup>. Rastogi *et al.* demonstrated that Nylon 46 can dissolve rapidly in superheated water at  $\sim 200\text{ }^{\circ}\text{C}$ , and re-crystallize on cooling<sup>[11, 12]</sup>. A hydrolysis process is hard to avoid when polyamides dissolved in superheated

<sup>\*</sup> This work was financially supported by the National Natural Science Foundation of China (No. 51373032), Innovation Program of Shanghai Municipal Education Commission, Fundamental Research Funds for the Central University and DHU Distinguished Young Professor Program. Z.W. thanks the support from Chinese Universities Scientific Fund (No. CUSF-DH-D-2014025).

<sup>\*\*</sup> Corresponding author: Shu-guang Yang (杨曙光), E-mail: shgyang@dhu.edu.cn

Received February 14, 2015; Revised April 25, 2015; Accepted April 25, 2015

doi:10.1007/s10118-015-1682-3

water. For Nylon 46 at 200 °C, 10 min after dissolution the molecular weight decreases considerably<sup>[12]</sup>. In supercritical water, PA 6 will decompose into  $\varepsilon$ -aminocaproic acid<sup>[13–17]</sup>.

In this work, we studied the hydrothermal processing of PA 6. The influences of hydrothermal temperature and processing time on dissolution and hydrolysis of PA 6 were investigated. We also discussed the hydrothermal annealing and the crystallization behavior in superheated water. After hydrothermal processing, the molecular weight of PA 6 was determined by intrinsic viscosity. The degree of hydrolysis of PA 6 at different temperatures and different times was estimated. It provides a temperature and time window for safe dissolving PA 6. It also provides useful information in recycling PA 6 by hydrothermal technology.

## EXPERIMENTAL

### Materials

PA 6 granules (Grade M2400), with a melt index of 26.0 g/10 min, were provided by Guangdong Xinhui Meida Nylon Co., Ltd.

### The Hydrothermal Processing of PA 6

Hydrothermal processing of PA 6 was carried in a 250 mL titanium autoclave (Weihai Chemical Machinery Co., Ltd. China) equipped with a magnetic stirrer, an electric heating jacket and an inside U-shaped pipe for cooling water. 5.65 g of virgin PA 6 granules and 200 mL deionized water were sealed in the autoclave. The pressures in the autoclave at different hydrothermal temperatures are listed in Table 1.

Heating the PA 6/water system to set temperatures required 30 min. After residence at the set temperature for different periods, the system was cooled down by circulating water. The solid samples in the reactor were collected and dried in a vacuum oven at 40 °C for 12 h.

**Table 1.** Temperature and corresponding pressure in the autoclave

Temperature (°C)	140	150	160	170	180	190	200
Pressure (MPa)	0.34	0.46	0.58	0.76	0.98	1.23	1.56

### Molecular Weight Determination after Hydrothermal Processing

Viscosity measurements were conducted in 85% formic acid solution with 10 mg·mL<sup>-1</sup> concentration by an Ubbelohde viscometer ( $\Phi = 0.5\text{--}0.6$  mm) at  $(25 \pm 0.1)$  °C. Relative viscosity ( $\eta_r$ ) and specific viscosity ( $\eta_{sp}$ ) were determined using the following equations:

$$\eta_r = t/t_0 \quad (1)$$

$$\eta_{sp} = \eta_r - 1 \quad (2)$$

where  $t$  and  $t_0$  are the efflux time of polymer solution and solvent, respectively. Experiments were repeated five times for all sample solutions. The intrinsic viscosity  $[\eta]$  was calculated based on the Maron equation<sup>[18]</sup>:

$$[\eta] = \frac{\eta_{sp} + \gamma \ln \eta_r}{(1 + \gamma)c} \quad (3)$$

where  $\gamma \approx 2$ <sup>[19]</sup>. The relationship between intrinsic viscosity and molecular weight was described by the Mark-Houwink equation:

$$[\eta] = KM_n^\alpha \quad (4)$$

$[\eta]$  is the intrinsic viscosity,  $M_n$  is the viscosity-average molecular weight,  $K$  is a constant, and  $\alpha$  is an exponent.  $K$  and  $\alpha$  depend on solvent and temperature. In 85% formic acid at 25 °C,  $\alpha = 0.82$  and  $K = 2.26 \times 10^{-4}$  dL·g<sup>-1</sup> for PA 6<sup>[20]</sup>.

### Differential Scanning Calorimetry (DSC)

DSC characterization was carried out on a NETZSCH 204F1 DSC. Two different sets of DSC were made. In one set of experiment, the conditions resembling those in the autoclave were reproduced. DSC was also used to characterize the initial and final products after the hydrothermal treatment.

In the first set of experiments, a 60  $\mu\text{L}$  stainless steel high-pressure pan was used for PA 6/water system. 15.0 mg of virgin PA 6 resin and 30  $\mu\text{L}$  of water were mixed and sealed in a stainless steel pan. A stainless steel pan with 30  $\mu\text{L}$  of water was used as a reference. The system was heated from 10  $^{\circ}\text{C}$  to 200  $^{\circ}\text{C}$ , hold at 200  $^{\circ}\text{C}$  for 5 min, and cooled down to 10  $^{\circ}\text{C}$  at 10  $\text{K}\cdot\text{min}^{-1}$ .

Aluminum pans were used to characterize the initial virgin PA 6 and the samples after hydrothermal processing. The pan contained 5–6 mg sample, and a blank aluminum pan was used as the reference. All the samples were heated from 10  $^{\circ}\text{C}$  to 250  $^{\circ}\text{C}$ , hold at 250  $^{\circ}\text{C}$  for 5 min, cooled to 10  $^{\circ}\text{C}$ , hold at 10  $^{\circ}\text{C}$  for 5 min, and heated to 250  $^{\circ}\text{C}$ . Heating and cooling rates were always 10  $\text{K}\cdot\text{min}^{-1}$ . The crystallinity was calculated using a heat of fusion of 243  $\text{J}\cdot\text{g}^{-1}$  for  $\alpha$  crystal<sup>[21]</sup>.

### FTIR Spectroscopy

FTIR spectra were recorded with a Nicolet 8700 spectrometer (Thermo Scientific). The PA 6 samples after hydrothermal processing were grinded into powder, mixed with the KBr powder at 1.0 wt%, and pressed into the standard disc for IR measurements (from 4000  $\text{cm}^{-1}$  to 400  $\text{cm}^{-1}$ , 64 scans, 4  $\text{cm}^{-1}$  resolution).

### WAXD and SAXS

Wide-angle X-ray diffraction (WAXD) measurements were carried out with Bruker D2 Desktop (Cu-K $\alpha$  0.15418 nm, 30 kV and 10 mA) and Bruker D8 Discover diffractometers (Cu-K $\alpha$  0.15418 nm, 40 kV and 40 mA, VÅNTEC-500 area detector), depending on the sample shape and morphology. The small angle X-ray scattering (SAXS) patterns of samples placed in two pieces of aluminum foil were measured in vacuum at room temperature with a SAXSess mc<sup>2</sup> instrument (Anton Paar GmbH, Austria), using line-collimated CuK $\alpha$  radiation (0.15418 nm) and an image plate detector. The scattering of the aluminum foil was subtracted as background. Background subtraction and correction for instrumental broadening were performed using the SAXS quant software.

## RESULTS AND DISCUSSION

DSC is a very convenient tool that provides an overall view of molecular and structure smooth kinetics of materials. A comparison of pure PA 6 with PA 6 processed hydrothermally (in the present of water, in a closed cell) is made. In both cases, initial melting, recrystallization on cooling and second melting have been performed. The corresponding curves are shown in Fig. 1.

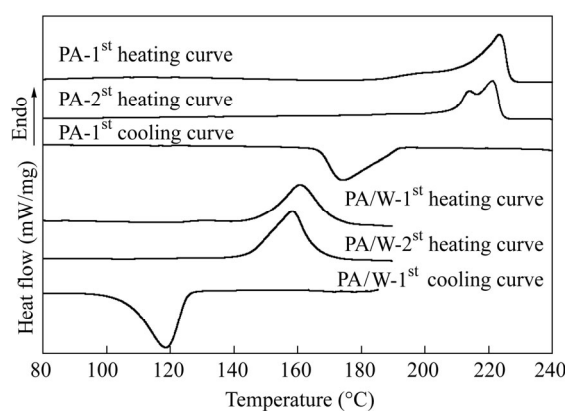


**Fig. 1** First heating, first cooling and second heating DSC curves of virgin PA 6 in aluminum pan (up) and PA 6/water in stainless steel pan (down)

In the first heating curve of the virgin PA 6, the melting peak is at 223 °C, and there is small shoulder on its lower temperature side. In the first cooling curve, the crystallization exothermal peak takes place at 174 °C. In the second heating curve, double melting peaks appear at 222 °C and 214 °C. Double melting peaks are very common for polyamides. They reflect the melting of thinner crystals and the reorganized thicker crystals<sup>[22, 23]</sup>. For the PA 6/water system, there is an endothermal peak located at 161 °C on the first heating curve that shifts to 158 °C on the second heating curve. In the cooling process the exothermal peak is at 119 °C.

The endothermal peak around 160 °C in DSC curve for the PA 6/water system corresponds to the dissolution process of PA 6 in superheated water, which is about 60 K lower than the melting of the virgin PA 6 under ambient condition. Also, the crystallization temperature of PA 6 from aqueous solution decreases compared with that from the melt.



**Fig. 2** Morphology of the PA 6 samples recovered from hydrothermal treatment with different conditions (For example, 140 °C-12 h means hydrothermal processing at 140 °C for 12 h.)

The dissolution process of PA 6 in superheated water is a process in which water molecules break the hydrogen bonding between amide groups in PA 6 and then make PA 6 dissolve in superheated water<sup>[11, 12]</sup>. It was reported that the Brill transition temperature ( $T_B$ ) of PA 6 was 160 °C<sup>[24, 25]</sup>, which should be helpful for the PA 6 dissolution in water. During the Brill transition process, PA 6 experienced a process of structural transformation from monoclinic to pseudo-hexagonal phase. Above  $T_B$ , there is a conformational disorder in the methylene

segments and a weakening of the hydrogen bonding in the crystal region of PA 6. In superheated water, due to the weakening of hydrogen bonding around the Brill transition temperature, the water molecules can easily break the hydrogen bonds and dissolve PA 6.

The high-pressure DSC indicated that the endothermal event starts already at about 140 °C in super-heated water, and hence 140 °C is taken in the present investigation as the lowest temperature limit to the hydrothermal process. The morphologies of PA 6 granulates after hydrothermal treatment in the 140–160 °C range for different times are exhibited in Fig. 2.

Between 140 °C and 155 °C, the granules keep their original shape but the semi-transparent surface gradually transforms into milky white. As the temperature increases (157–159 °C), most of the particles no longer maintain their original shape and some bulk solid blocks start to form, which imply PA 6 starts to dissolve from surface. At 160 °C, hydrothermal treatment completely changes the resin shape. After 1 h the resin displays curved sheets and after 12 h the resin is made of small pieces. After 24 h, the recovered PA 6 resin is made of lumps that can easily be grinded into powder. It indicates that at 160 °C PA 6 resin gradually dissolves in water. These morphological changes are accompanied by a significant weight loss, *i.e.* by hydrolysis of the PA 6. Out of the 5.65 g PA 6 initially introduced in the autoclave, 5.22 g, 4.65 g and 4.37 g PA 6 were recovered after 1 h, 12 h and 24 h processing at 160 °C respectively. This significant weight decrease indicates that PA 6 is hydrolyzed when dissolved in super-heated water.

#### **PA 6 Annealing below 160 °C in the Hydrothermal Treatment**

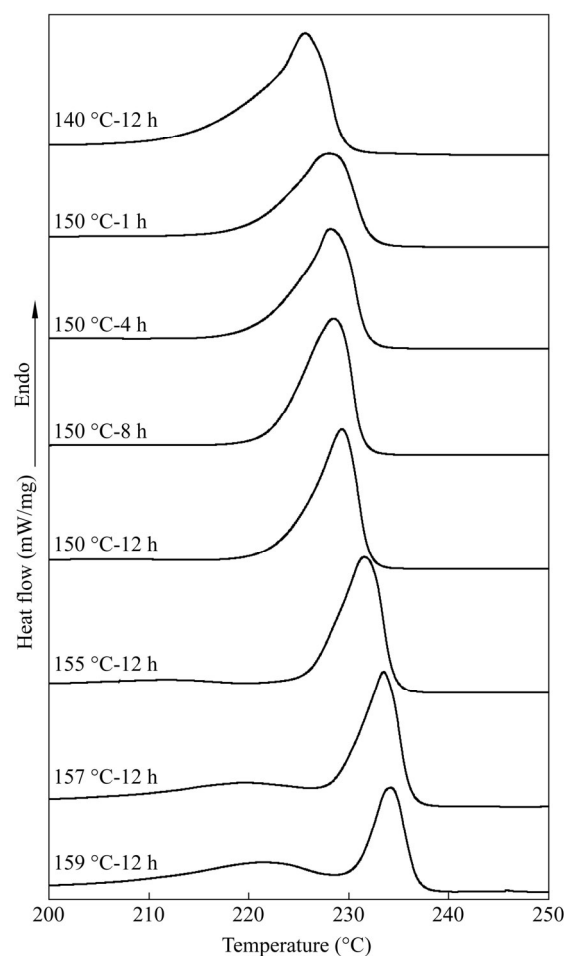
$T_m$  of the virgin PA 6 (223 °C) provides the reference that helps establish the impact of temperature and water on the thickening of the lamellae. Annealing in the temperature range (140–159 °C) is expected to induce lamellae thickening, which is demonstrated by the melting temperature ( $T_m$ ) elevation of the sample after hydrothermal treatment and the changes in the SAXS profile. Murthy *et al.* reported that water can diffuse into the amorphous region, which increases the mobility of PA 6 chains and is helpful for chain rearrangement and lamellae thickening<sup>[26, 27]</sup>.

Figure 3 summarizes the DSC data for various  $T_H < 160$  °C as a function of time. The melting curve of  $T_H = 140$  °C is virtually identical (including peak position) to that of virgin PA 6 (223 °C). Only the lower end of the peak has shifted to higher temperature probably due to annealing of the least stable crystals. As  $T_H$  increases to 159 °C, the  $T_m$  shifts to 234 °C. It also becomes narrower with increasing  $T_H$  and residence time (compare the curves of samples after processed at 150 °C for different time). The increase of melting temperature indicates lamellae thickening. However, a faint peak at ~210–220 °C starts to appear for  $T_H = 155$  °C, which becomes more prominent for  $T_H = 157$  °C and 159 °C. Anticipating later results, this peak corresponded to the surface material that has dissolved and then recrystallized as the temperature down. And the later results show that the PA 6 crystallized from water has the lower melting peak.

For the virgin PA 6 granules, a broad peak is present at  $q = 0.76 \text{ nm}^{-1}$ . After annealing at 140 °C for 12 h, the peak shifts to lower  $q$ , which indicates that lamellae become thick. The average lamellar thickness of the virgin PA 6 is estimated to be 8.3 nm, while after annealing at 140 °C for 12 h, the average thickness is about 10.7 nm. However, this thickening degree does not make obvious melting temperature increasing.

Gogolewski *et al.* investigated the crystallization of PA under ultra-high pressure<sup>[28–32]</sup>. PA 6 crystallized isothermally at 215 °C under atmospheric pressure for 48 h has a melting temperature of 225 °C and a lamellae thickness of 7 nm. PA 6 crystallized at 230 °C under 150 MPa for 36 h has the same melting temperature, but its lamellae thickness increased to 19 nm. However, the sample crystallized at 245 °C under 350 MPa for 72 h presents the melting peak at 234 °C and the lamellae thickness is 100 nm, which is determined from electron microscope picture by measuring the step heights in the fracture surface.

As shown in Fig. 4, SAXS peak does not present for  $T_H \geq 150$  °C. The SAXS profile reflects the space correlation function of electric charge density variation. The melting temperature elevating indicates lamellae thickening. The main reason for no peak in SAXS should be that there is no order for lamellae packing.



**Fig. 3** First heating curves of samples after processing below 160 °C in superheated water for different periods

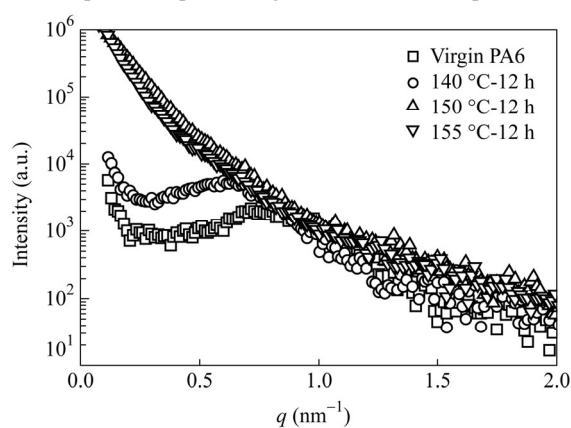


**Fig. 4** The SAXS profiles of samples

#### **Hydrothermal Treatments in the 160 °C–200 °C Range**

All hydrothermal treatments performed at and above 160 °C imply complete dissolution and recrystallization of the PA 6. Figure 5(a) displays the DSC melting curves of the PA 6 crystallized from the superheated solution, recovered and dried as a function of temperature and time (for the sole 160 °C hydrothermal process) and Fig. 5(b) displays the second heating curves.

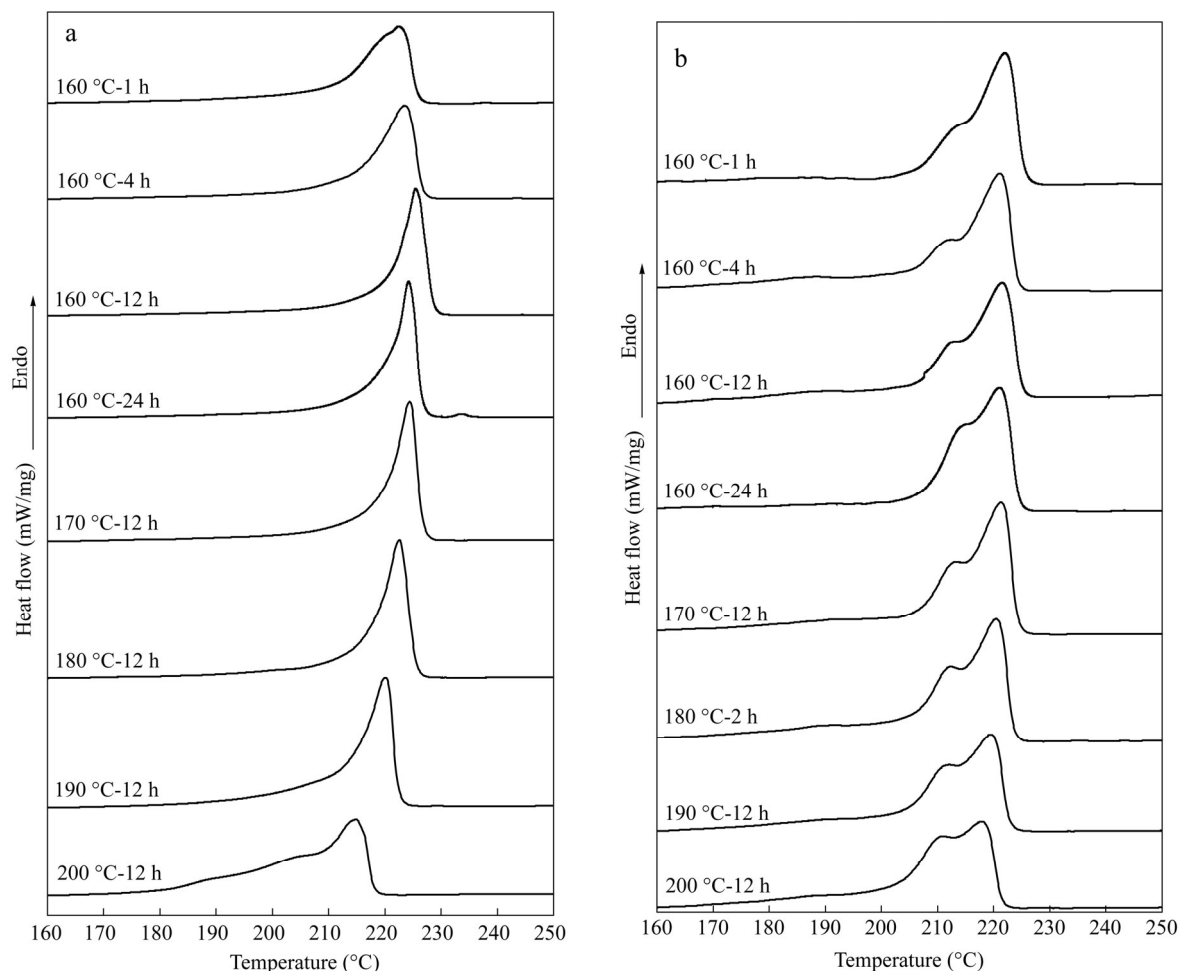


**Fig. 5** (a) The first and (b) the second heating curves of samples after processing above or at 160 °C in superheated water, recorded in nitrogen atmosphere at 10 K·min<sup>-1</sup>

In the first heating, the melting temperatures have dropped considerably compared to those after the hydrothermal process at 159 °C. This drop is the signature of crystallization from the solution, as opposed to annealing of a sample in the solid state. The melting bands of the samples treated at 160 °C became narrow with increasing residence time and the second peak (or shoulder) below the major peak disappeared after 1 h residence.

Whereas hydrothermal treatments at higher temperatures yield sharp peaks, the maximum shifts progressively to lower temperatures. At the same time, the peaks become asymmetric, with a significant lower temperature tail. Residence at 200 °C for 12 h results in significant hydrolysis, as suggested by the large fraction of material melting at lower  $T_m$ .

The second heating curves display systematically two peaks. Such cases are typical of melt crystallized PA 6. However, the lower melting peak component become more prominent with increase of  $T_H$ , which indicates the strengthen impact of molecular weight reduction.

In all the reported experiments, the whole 140 °C to 200 °C, the  $\alpha$  phase crystal structure of the material remains unchanged. This is illustrated by both WAXS and FTIR results. The WAXS patterns (Fig. 6) displays two peaks at 20° (200) and 24° (002 + 202), which are feature peaks for the  $\alpha$  phase<sup>[33–35]</sup>. For  $\gamma$  phase of PA 6, there are peaks indexed as 001 and 200/201, present at 22° and 23° respectively. But, the 200/201 diffraction appears as a shoulder to the 001 diffraction peak. The FTIR spectrum confirms the  $\alpha$  phase (Fig. 7). The peaks at

928  $\text{cm}^{-1}$  and 959  $\text{cm}^{-1}$  (CO—NH in plane vibration), 1199  $\text{cm}^{-1}$  ( $\text{CH}_2$  twist-wag vibration), 1373  $\text{cm}^{-1}$  (amide III and  $\text{CH}_2$  wag vibration), 1416  $\text{cm}^{-1}$  and 1478  $\text{cm}^{-1}$  ( $\text{CH}_2$  scissors vibration) are all characteristics of the  $\alpha$  phase<sup>[36–39]</sup>.

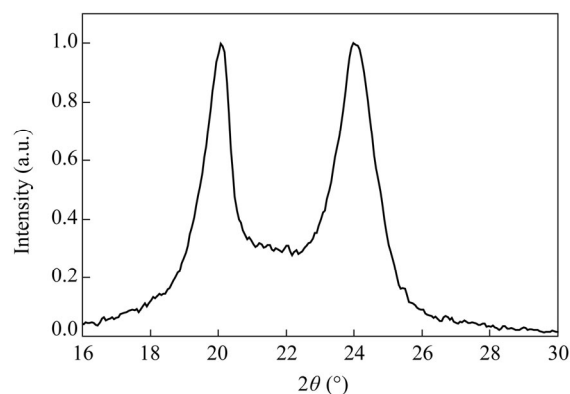


**Fig. 6** WAXD pattern of a PA 6 sample crystallized from the superheated water after hydrothermal processing at 200 °C for 12 h

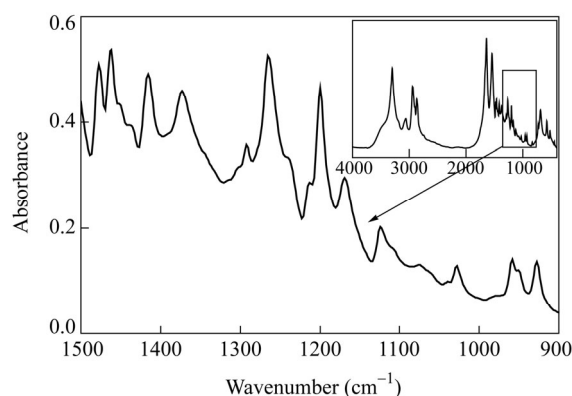


**Fig. 7** FTIR spectrum of a PA 6 sample crystallized from the superheated water after hydrothermal processing at 200 °C for 12 h

The hydrothermal processing in the temperature range 160–200 °C results in samples losing weight, but the higher crystallinity ( $X_c$ ) as  $T_H$  increases.  $X_c$  is ~29% in the virgin PA 6, but gradually reaches ~48% after the processing at 200 °C for 12 h. This higher crystallinity is due to the lower  $M_w$  of samples reached after the hydrothermal processing.

#### Hydrolysis of PA 6 during Hydrothermal Treatment

PA 6 hydrolyzes during the hydrothermal treatments above 160 °C. After hydrothermal processing the molecular weight of PA 6 was measured as a function of hydrothermal temperature and time. The  $M_w$  variation is shown in Fig. 8. Starting from an initial  $M_w$  of 21700, the decay of  $M_w$  at a hydrothermal temperature can be fitted with an exponential function:

$$M_w = A + B \exp\left(\frac{-t}{C}\right)$$

where  $A$ ,  $B$  and  $C$  are constants and  $t$  is the hydrothermal processing time.  $A$ ,  $B$  and  $C$  are dependent on the hydrothermal temperature. The  $M_w$  is reduced by about one half after 24 h residence at 160 °C. The decrease is spectacular at 200 °C, the  $M_w$  is reduced nearly tenfold to approximately 2000 in 8 h. It is also found that after reaching an asymptote value,  $M_w$  remains nearly constant afterwards which suggests that some form of equilibrium in a hydrolysis/recombination process. This possibility is demonstrated by the quasi-constancy of  $M_w$  approximately after 12 h when  $T_H = 190$  °C.

#### Defining an Acceptable Hydrolysis for PA 6 under Hydrothermal Condition

The data shown in Fig. 8 help establish the kinetics of PA 6 hydrolysis under hydrothermal conditions, and they yield the  $A$ ,  $B$  and  $C$  parameters of the exponential decay of the PA 6 molecular weight. These parameters in turn can be used to calculate the molecular weight decrease after various residence times in the hydrothermal process (Fig. 9). An immediate outcome would be to determine what conditions should be used to limit the molecular weight degradation of PA 6.



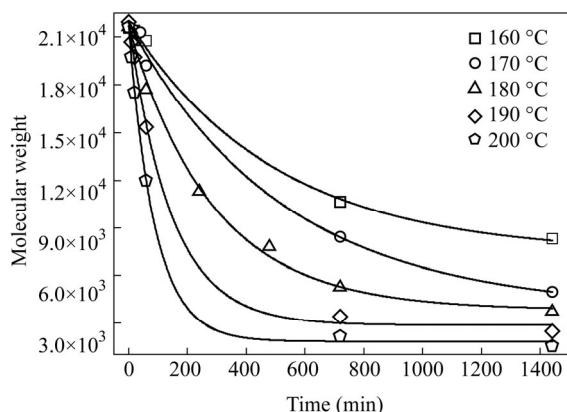


**Fig. 8** The exponential decay of the PA 6 molecular weight after hydrothermal processing for different time lengths at different temperatures

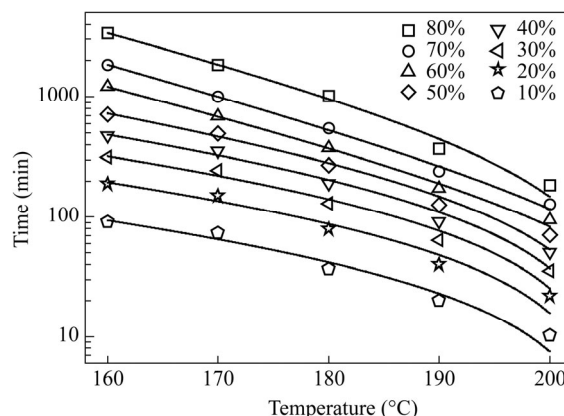


**Fig. 9** The molecular weight decrease after various residence times in the hydrothermal process

The hydrolysis cannot be neglected when the  $M_w$  decrease approximately 10% (*i.e.* the final  $M_w$  is 20000 as compared to the initial 21700). The resulting residence times at the various hydrothermal temperatures are also shown in Fig. 9. The fitting curve for these points then can be looked at as a boundary for the ‘safe’ dissolution of PA 6. Conversely, beyond this limit (or any other limit calculated for larger  $M_w$  decreases), one may define hydrothermal treatments that reduce  $M_w$  more drastically. It provides guide information for PA 6 recycling processes based on hydrothermal technology.

## CONCLUSIONS

PA 6 dissolves in superheated water above 160 °C, and crystallizes from the water solution when  $T < 120$  °C. Between 140 °C and 155 °C, PA 6 merely anneals. Lamellae thickness increases as reflected by a higher melting temperature. Between 157 °C and 159 °C, this annealing effect is maintained, but surface recrystallization and partial dissolution take place also. Above 160 °C, PA 6 dissolves completely in water but the hydrolysis sets in. As the temperature is elevated and processing time is extended, the hydrolysis becomes a major factor. The hydrolysis induced molecular weight decrease fits an exponential decay.

**ACKNOWLEDGEMENTS** We thank Prof. Bernard Lotz for discussion on Nylon crystal structure.

## REFERENCES

- 1 Tuzar, Z., Kratochvíl, P. and Bohdanecký, M., *Adv. Polym. Sci.*, 1979, 30: 117
- 2 Schroeder, L.R. and Cooper, S.L., *J. Appl. Phys.*, 1976, 47: 4310
- 3 Murthy, N.S., *J. Polym. Sci., Part B: Polym. Phys.*, 2006, 44: 1763
- 4 Bai, Y.P., Huang, L., Huang, T., Long, J. and Zhou, Y.F., *Polymer*, 2013, 54: 4171
- 5 Galkin, A.A. and Lunin, V.V., *Russ. Chem. Rev.*, 2005, 74: 21
- 6 Akiya, N. and Savage, P.E., *Chem. Rev.*, 2002, 102: 2725
- 7 Brunner, G.J., *Supercrit. Fluids*, 2009, 47: 373
- 8 Wevers, M.G.M., Mathot, V.B.F., Pijpers, T.F.J., Goderis, B. and Groeninckx, G., *Lect. Notes Phys.*, 2007, 714: 151
- 9 Wevers, M.G.M., Pijpers, T.F.J. and Mathot, V.B.F., *Thermochim. Acta*, 2007, 453: 67
- 10 Charlet, K., Mathot, V.B.F. and Devaux, J., *Polym. Int.*, 2011, 60: 119
- 11 Rastogi, S., Terry, A.E. and Vinken, E., *Macromolecules*, 2004, 37: 8825
- 12 Vinken, E., Terry, A.E., Van Asselen, O., Spoelstra, A.B., Graf, R. and Rastogi, S., *Langmuir*, 2008, 24: 6313

- 13 Ikushima, Y., Sato, O., Sato, M., Hatakeda, K. and Arai, M., *Chem. Eng. Sci.*, 2003, 58: 935
- 14 Iwaya, T., Sasaki, M. and Goto, M., *Polym. Degrad. Stab.*, 2006, 91: 1989
- 15 Goto, M.J., *Supercrit. Fluids*, 2009, 47: 500
- 16 Chen, J.Y., Liu, G.Y., Jin, L.J., Ni, P., Li, Z., He, H.B., Xu, Y., Zhang, J.Q. and Dong, J.P., *J. Anal. Appl. Pyrolysis*, 2010, 87: 50
- 17 Chen, J.Y., Li, Z., Jin, L.J., Ni, P., Liu, G.Y., He, H.B., Zhang, J.Q., Dong, J.P. and Ruan, R.Y., *J. Mater. Cycles Waste Manage.*, 2010, 12: 321
- 18 Maron, S.H., *J. Appl. Polym. Sci.*, 1961, 5: 282
- 19 Kohan, M.I., in "Nylon plastics handbook", Hanser Publishers, New York, 1995, p. 80
- 20 Mattiussi, A., Gechele, G.B. and Francesconi, R., *J. Polym. Sci. A-2 Polym. Phys.*, 1969, 7: 411
- 21 Vlasveld, D.P.N., Groenewold, J., Berseec, H.E.N., Mendes, E., and Picken, S.J., *Polymer*, 2005, 46: 6102
- 22 Franco, L. and Puiggali, J., *J. Polym. Sci., Part B: Polym. Phys.*, 1995, 33: 2065
- 23 Wang, G.M., Yan, D.Y. and Bu, S.H., *Chinese J. Polym. Sci.*, 1998, 16(3): 241
- 24 Murthy, N.S., Curran S.A., Aharoni, S.M. and Minor, H., *Macromolecules*, 1991, 24: 3215
- 25 Vasanthan, N., Murthy, N.S. and Bray, R.G., *Macromolecules*, 1998, 31: 8433
- 26 Murthy, N.S., Stamm, M., Sibilia, J.P. and Krimm, S., *Macromolecules*, 1989, 22: 1261
- 27 Murthy, N.S. and Akkapeddi, M.K., *Macromolecules*, 1998, 31: 142
- 28 Gogolewski, S. and Pennings, A.J., *Polymer*, 1973, 14: 463
- 29 Gogolewski, S. and Pennings, A.J., *Polymer*, 1975, 16: 673
- 30 Gogolewski, S. and Pennings, A.J., *Polymer*, 1977, 18: 647
- 31 Gogolewski, S. and Pennings, A.J., *Polymer*, 1977, 18: 654
- 32 Gogolewski, S., *Polymer*, 1977, 18: 63
- 33 Arimoto, H., Ishibashi, M., Hirai, M. and Chatani, Y., *J. Polym. Sci. Part A*, 1965, 3: 317
- 34 Ramesh, C. and Gowd, E.B., *Macromolecules*, 2001, 34: 3308
- 35 Zhong, L.W., Ren, X.K., Yang, S., Chen, E.Q., Sun, C.X., Stroeks, A. and Yang, T.Y., *Polymer*, 2014, 55: 4332
- 36 Rotter, G. and Ishida, H., *J. Polym. Sci., Part B: Polym. Phys.*, 1992, 30: 489
- 37 Arimoto, H., *J. Polym. Sci. A Gen. Pap.*, 1964, 2: 2283
- 38 Tobin, M.C. and Carrano, M.J.J., *Chem. Phys.*, 1956, 25: 1044
- 39 Wu, Q., Liu, X. and Berglund, L.B., *Polymer*, 2002, 43: 2445